Int. J. Solids Structures, 1971, Vol. 7, pp. 445 to 458. Pergamon Press. Printed in Great Britain

IMPACT ON PLATES AND SHELLS

JACKSON C. S. YANG†

U.S. Naval Ordnance Laboratory, White Oak, Maryland

Abstract—Theoretical relations and experimental data for the collision of spherically-headed projectiles with hemispherical shells and square plates with and without protective coverings are presented. An extension of the Hertz static contact problem and the Hertz force–indentation law combined with plate and shell theories give theoretical relations for the calculations of the stress distribution. The theoretical predictions were verified experimentally by using an air gun to impact spherically-headed steel projectiles on glass and aluminum hemispherical shells, and steel and aluminum square plates with and without viscoelastic (polyurethane) and plastic (polycarbonate) coverings. Strain measurements were taken from strain gages mounted on the free side of the plate or shell, directly under the point of impact. Reasonable agreement between the results of the calculations and the experimental data was obtained.

NOTATION

a, b	lateral dimensions of the plate, in.
c	radius of contact, in.
D	flexural rigidity
E	Young's modulus of elasticity, psi
h	thickness of the plate, in.
J_1	Bessel function of order one
m_2	mass of projectile, lb sec^2/in.
M	mass of cladded sphere
M_x, M_y	bending moments, lb-in.
M_{xy}	twisting moment, lb-in.
n	constant dependent upon the materials and dimensions of two bodies
P	compressive force, lb.
q	intensity of contact pressure, psi
q_0	maximum contact pressure, psi
R	radius of glass hemisphere
R_1, R_2	radii of two contact bodies, in.
t	thickness of glass hemisphere
T_{xy}	shearing stress, psi
v	velocity of impact, fps
v_1, v_2	velocities of two bodies after contact, fps
W	deflection of the plate, in.
α	relative indentation, in.
ν	Poisson's ratio
σ_0	membrane stress
σ_B	bending stress
σ_c	combined stress
σ_x, σ_y	bending stresses, psi

INTRODUCTION

DURING the past decade increasing attention has been focused on the problems attendant to the collision of a projectile and a target. The first attempt to incorporate a theory of local indentations was based on a scheme suggested by Hertz [1], who viewed the contact

† Associate Professor, Mechanical Engineering Department, University of Maryland.

of two bodies as an equivalent problem in electrostatics. A solution was obtained in the form of a potential which described the stresses and deformations near the contact point as a function of the geometrical and elastic properties of the bodies. This result, although both static and elastic in nature, has been widely applied to impact situations where permanent deformations were produced. The use of the Hertz law under dynamic conditions has been justified on the basis that it appears to predict accurately most of the impact parameters that can be experimentally verified. Davis [2] indicates that for the case of impact of elastic bodies at moderate velocities the problems of elastic contact and elastic impact are in essence identical. Love [3] and Tsai and Kolsky [4] indicate that the quasi-static treatment is found to approximate very closely the values of stress found in dynamic impacts. Raman [5] applied the Hertz theory to the investigation of the coefficient of restitution and found that for moderate plate thicknesses (0·138–1 in.) the theoretically calculated and experimentally observed values agreed well. In further investigations Goldsmith [6] extended his experimental observations to intermediate velocities (30–300 ft/sec) of impact, using the Hopkinson bar technique, and he vindicated the use of the Hertz law for hard tool steel, even when some permanent set was produced; however, he rejected its application to aluminum.

For the purpose of determining the validity of applying the Hertz static treatment and the Hertz force–indentation law to thin plates and shells under intermediate velocities of impact, the present paper gives an analytical solution for the stress distribution of the plate and shell under transverse impact.

A comparison is then made with experimental data obtained by using an air gun to impact spherically-headed steel projectiles with different radii of curvature against aluminum and glass hemispherical shells, and aluminum and steel square plates of various thicknesses, with and without viscoelastic (polyurethane–Adiprene) and plastic (polycarbonate–Lexan) coverings. The shock mitigation properties of the two cladding materials, Adiprene and Lexan, were also obtained.

THEORETICAL ANALYSIS

For the impact between two spheres of mass m_1 and m_2, investigations show that the duration of impact, i.e. the time during which the spheres remain in contact, is very long in comparison with the period of the lowest mode of vibration of the spheres [7]. Vibrations can therefore be neglected and it can be assumed that the force–displacement relation established for static conditions holds during impact.

The total force P resisting the impact motion of the cladded plate and shell is given by Hertz's contact law:

$$P = nx^{\frac{3}{2}}, \tag{1}$$

where x is the total deflection of the cladding and n is a stiffness coefficient determined by the dimensions and the elastic–plastic properties of the cladding material. The constant n is given by:

$$n = \frac{4}{3\pi(k_1+k_2)}\left(\frac{R_1R_2}{R_1+R_2}\right)^{\frac{1}{2}}, \tag{2}$$

where R_1 and R_2 are the radii of the spherical surfaces of the two bodies at the point of contact, and

$$k_1 = \frac{1-v_1^2}{\pi E_1}, \qquad k_2 = \frac{1-v_2^2}{\pi E_2},$$

in which E and v are Young's modulus and Poisson's ratio, respectively. This is similar to considering the material as a nonlinear spring.

For the problem of impact on plates, equation (2) may be simplified to

$$n = \frac{4R_2^{\frac{1}{2}}}{3\pi(k_1+k_2)}, \tag{3}$$

in which subscripts 1 and 2 represent plate and projectile, respectively. During the impact of such a system the following differential equation may be written:

$$m_2\ddot{x} + nx^{\frac{3}{2}} = 0. \tag{4}$$

The solution of the differential equation gives the displacement, velocity and acceleration of the spherical nosed projectile as functions of time. With the displacement of the spherical projectile known, the force acting on the plate at any time can be obtained from equation (1).

The maximum force acting on the plate and shell is obtained when the displacement of the projectile is at a maximum.

$$P_{\max} = nx_{\max}^{\frac{3}{2}} \tag{5}$$

The maximum compression of the cladding and the duration of impact can be determined directly by requiring the work done by the cladding to equal the kinetic energy of the system. The indentation of the plate and shell is neglected since it is very small when compared to the deflection of the cladding. In this case:

$$x_{\max} = \left(\frac{5}{4}\frac{M_2}{n}V_0^2\right)^{\frac{2}{5}} \tag{6a}$$

and

$$t_d = \frac{2X_{\max}}{v_0}\int_0^1 \frac{\mathrm{d}x}{\sqrt{[1-(x)^{\frac{5}{2}}]}} \approx 2{\cdot}94\frac{X_{\max}}{v_0} \tag{6b}$$

Substituting the equation for $x_{\max}$ into equation (5), the maximum force acting on the plate and shell is obtained as:

$$P_{\max} = n\left(\frac{5}{4}\frac{M_2}{n}V_0^2\right)^{\frac{3}{5}} \tag{7}$$

Thus far in the analysis, the deflection of the plate and the shell is neglected. However, for thin plates and shells, the bending should be taken into consideration. In Ref. [7] a differential equation of motion was written for an approximate solution to the case of the central transverse impact of a sphere on a rectangular plate simply supported along all edges.

$$\frac{\mathrm{d}^2x}{\mathrm{d}t^2} + \frac{1}{m}P(x) + \frac{1}{16b^2}\left[\frac{3(1-v^2)}{\rho E}\right]^{\frac{1}{2}}\frac{\mathrm{d}}{\mathrm{d}t}P(x) = 0 \tag{8}$$

The elastic force–indentation law, equation (1), is now employed to eliminate the term $P(x)$ from the equation. Introducing a dimensionless variable defined by

$$\bar{x} = \frac{x}{\bar{T}v_0}, \qquad \bar{t} = \frac{t}{\bar{T}} \tag{9}$$

Equation (9) may be written as

$$\frac{d^2x}{dt^2} + \left[1 + \bar{\lambda}\frac{d}{d\bar{t}}\right]\bar{x}^{\frac{3}{2}} = 0 \tag{10}$$

with

$$\bar{x} = 0, \qquad \frac{dx}{d\bar{t}} = 1 \text{ for } \bar{t} = 0$$

where T, a constant with dimensions of time, is so chosen that the first two coefficients in the transformed equations are unity. This condition requires that

$$\bar{T} = \left[\frac{m}{k_2 v_0^{\frac{1}{2}}}\right]^{\frac{2}{5}} = 0{\cdot}311 t_H \text{ and } \bar{\lambda} = \frac{1}{16b^2}\left[\frac{3(1-v^2)}{\rho E}\right]^{\frac{1}{2}} \frac{m}{\bar{T}} \tag{11}$$

where t_H is the Hertzian duration of contact for a plate of infinite thickness. For a striking sphere of radius R, the parameter $\bar{\lambda}$ is given by

$$\bar{\lambda} = \frac{\pi^{0{\cdot}6}}{3^{0{\cdot}5}}\left(\frac{R}{2b}\right)^2\left(\frac{\rho_2}{\rho_1}\right)^{0{\cdot}6}\left\{\frac{v_0}{\sqrt{[E_1/\rho_1(1-v_1^2)]}}\right\}^{0{\cdot}2}\left[\frac{E_2/(1-v_2^2)}{E_1E_2/(1-v_1^2)(1-v_2^2)}\right]^{0{\cdot}4} \tag{12}$$

For plates with cladding:

$$\bar{\lambda} = \frac{1}{16b^2}\left[\frac{3(1-v_1^2)}{\rho_1 E_1}\right]^{0{\cdot}5} m_2^{0{\cdot}6} v_0^{0{\cdot}2}\left\{\frac{4}{3}\frac{R^{0{\cdot}5}}{(1-v_2^2)/E_2 + (1-v_3^2)/E_3}\right\}^{0{\cdot}4} \tag{13}$$

where subscripts $_1$, $_2$ and $_3$ denote the plate, the spherical projectile, and the cladding, respectively.

The results of numerical integrations of equation (10) for various values of $\bar{\lambda}$ are shown in Fig. 1 for dimensionless displacement histories $x/\bar{T}v_0$ as a function of dimensionless time $t/\bar{T}$ from Hertz contact force law. This gives us the force P acting on the plate at any time having taken into consideration the bending of the plate.

According to Hertz, the intensity of pressure q over the surface of contact is represented by the ordinates of a hemisphere of radius c constructed on the surface of contact. The peak bearing stress is obtained by equating the sum of the pressures over the contact area to the compressive force P. For a hemispherical pressure distribution this stress can be written as a function of displacement

$$q_0 = \frac{E}{\pi(1-v^2)}\left(\frac{x_{\max}}{R_2}\right)^{\frac{1}{2}} \tag{14}$$

Knowing the bearing stress and the material properties of the plate, shell and the cladding, the bending stress and inertia in the plate can be calculated for the case of a small circular area of bearing stress on the plate by the thin plate theory (9), and the combined stresses in the shell can be calculated for the case of a small circular area of bearing stress on the apex of the shell by the shell theory of Reissner (10).

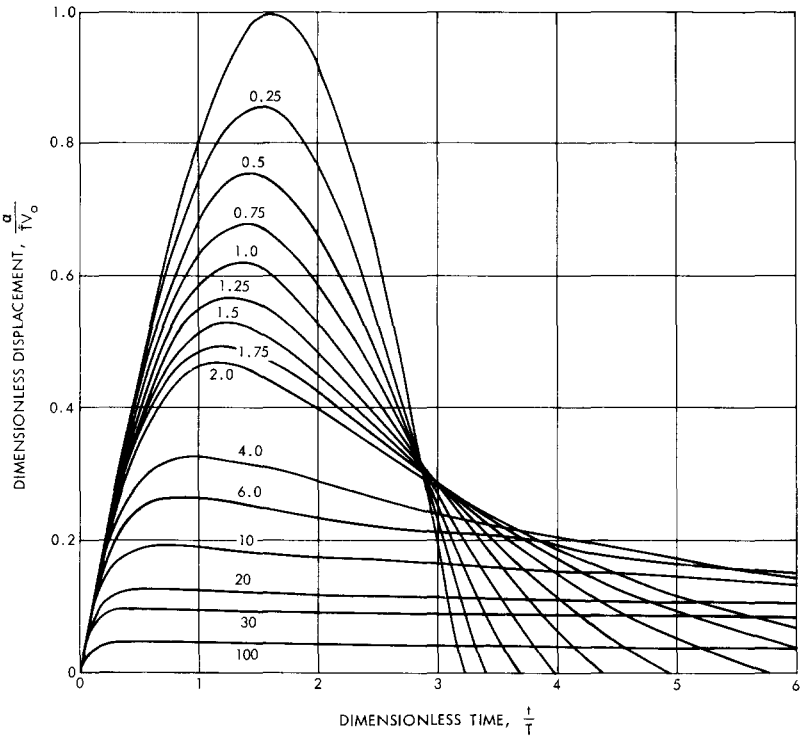

FIG. 1. Dimensionless displacement as a function of dimensionless time.

Equations for stresses

1. *Hemispherically distributed contact pressure on plate.* For a square plate the maximum bending moments occur at the center of the plate and the maximum bending stresses at the surfaces, we have (see Ref. [9] and Fig. 2)

$$\sigma_{x\max} = \sigma_{y\max} = \frac{6a^2}{(2b)^2\pi^2} \sum_{m=1,3,5}^{\infty} \sum_{n=1,3,5}^{\infty} \frac{A_{mn}(m^2 + \nu n_2)}{(m^2+n^2)^2} (-1)^{[m+n)/2]-1} \tag{15}$$

$$\tau_{xy} = 0 \tag{16}$$

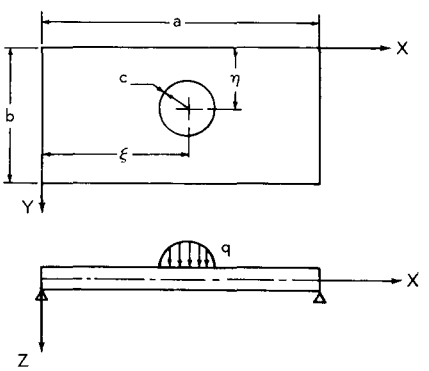

FIG. 2. Hemispherically distributed contact pressure.

where

$$A_{mn} = \frac{GF}{ab\pi c^3} \int_0^c \int_0^{2\pi} \sqrt{(c^2 - r^2)} \sin \frac{m\pi(\xi + v\cos\theta)}{a} \sin \frac{n\pi(n + v\sin\theta)}{b} r \, dr \, d\theta \tag{17}$$

2. *Uniformly distributed contact pressure on plate.* Tsai and Kolsky [4] found in the study of wave propagation that a theoretical analysis gave close agreement with the experimental pulse shapes, by assuming that the area of contact has a finite radius, and stress is distributed uniformly over this circular area. Therefore, for the simplification of the problem, we can assume that the compressive force is uniformly distributed over the contact area as shown in Fig. 3.

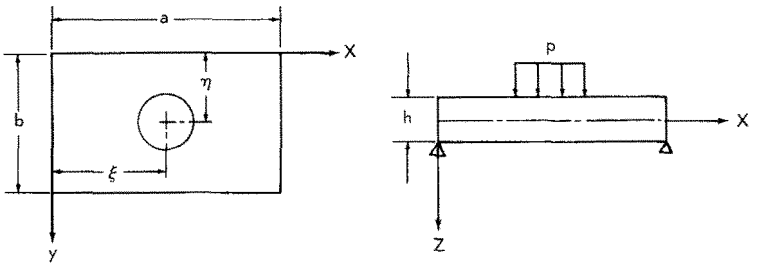

FIG. 3. Uniformly distributed contact pressure.

As in the previous section, the stress at the center of the surface of the plates: (see Ref. [9] and Fig. 3).

$$\sigma_{x\max} = \sigma_{y\max} = \frac{48Fa}{\pi^3(2b)^2 c} \sum_{m=1,3,5}^{\infty} \sum^{\infty} \frac{J_1(\gamma_{mn}C)(-1)^{m+n}(m^2 + vn^2)}{(m^2 + n^2)^{\frac{5}{2}}} \tag{18}$$

$$\tau_{xy} = 0 \tag{19}$$

3. *Uniformly and hemispherically distributed contact pressure on shell.* The combined stress can be calculated for the inner and the outer surface of the glass and aluminum shell at the pole by the use of the shallow shell theory of Reissner [10]. The pole was selected since we are primarily interested in the maximum tensile stress in the glass and aluminum shell. With the notation of Figs. 4 and 5 the explicit expressions for stresses at the apex of the shell for a uniformly distributed load of magnitude F bounded by a circle of radius a is given by:

$$\sigma_D(0) = -\frac{\sqrt{[12(1-v^2)]}}{2\pi} \frac{F}{t^2} \left(\frac{ker'\mu}{\mu} + \frac{1}{\mu^2} \right) \tag{20}$$

$$\sigma_B(0) = \pm \frac{3(1+v)}{\pi} \frac{F}{t^2} \frac{kei'\mu}{\mu} \tag{21}$$

where $ker'\mu$ and $kei'\mu$ are the real and imaginary parts of Kelvin functions and a prime represents differentiation with respect to μ. Also

$$\mu = \frac{\sqrt[4]{[12(1-v^2)]}(a)}{Rt}$$

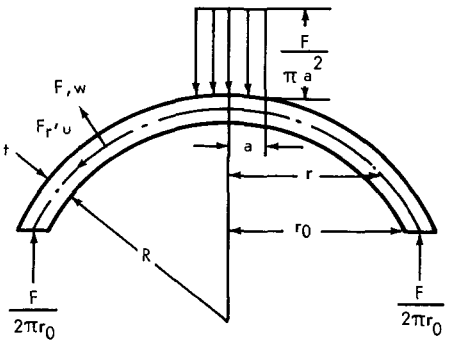

FIG. 4. Uniformly distributed stress on glass shell.

The combined stress at the apex of the shell becomes

$$\sigma_c(0) = \sigma_D(0) + \sigma_B(0), \tag{22}$$

and thus

$$\sigma_c(0) = \mp\frac{3(1+\nu)}{\pi}\frac{F}{t^2}\frac{kei'\mu}{\mu} - \frac{\sqrt{[12(1-\nu^2)]}}{2\pi}\frac{F}{t^2}\left(\frac{ker'\mu}{\mu} + \frac{1}{\mu^2}\right)$$

For a hemispherical stress distribution, we sliced the hemisphere into many layers. Each layer can be considered to have uniformly distributed loading with corresponding stresses which can be summed to give the total bending and membrane stresses.

Test specimens and coverings

Steel and aluminum square plate (6 × 6 in.) in various thicknesses, strengthened glass shells, 0·2875 in. thick, 5·00 in. in radius and mass of 0·144 slug, and Adiprene (h–0·29 in.) and Lexan (h–0·19 in.) coverings were used. Rockwell hardness tests were carried out to obtain the mechanical properties of steel, and the results were interpreted using the ASM Handbook [11].

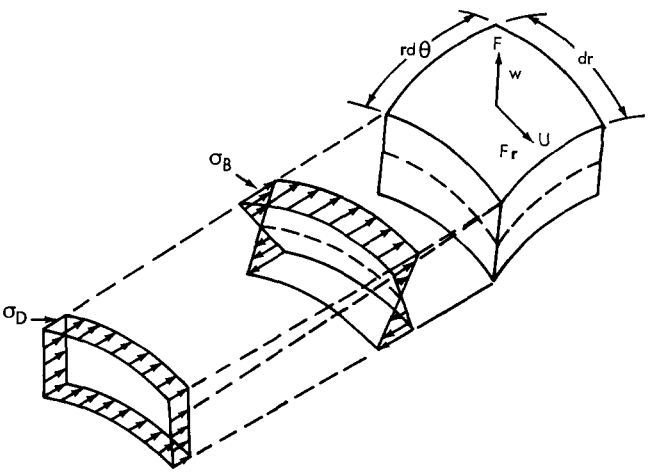

FIG. 5. Stresses at apex of glass shell.

The mechanical properties of the specimens and coverings are listed in the following Table.

TABLE 1. MECHANICAL PROPERTIES OF SPECIMENS AND COVERINGS (SPECIMENS: $6 \times 6 \times 0{\cdot}375$ in.)

Materials	Modulus of elasticity E (psi)	Poisson's ratio	Hardness R_b	Tensile strength (ksi)	Yield strength (ksi)
Aluminum alloy	$10{\cdot}3 \times 10^6$	0·33	80	82	70
Steel, carbon and alloy	30×10^6	0·30	74	63	35
Adiprene	50×10^3†	0·45			
Lexan	320×10^3†	0·37			
Glass	$10{\cdot}5 \times 10^6$†	0·2122			

† These values were obtained from [12] by taking an average value of E for various strain rates.

EXPERIMENTAL TECHNIQUE

Two steel projectiles having 0·5 and 1·0 in. radii spherical heads were fired from an air gun using pressures between 25 and 65 psi. Velocities up to 85 ft/sec were obtained. A frequency counter connected to two photocells placed 2 in. apart timed the passage of the projectile in microseconds. Strain measurements were made with foil strain gages mounted on the free side of the plate and the shell directly under the point of impact, and connected to an oscilloscope. An oscilloscope with a fast rise time and a trigger delay circuit was used to display the output of the gage. The lower of the two photocells was used to trigger the oscilloscope through a delay circuit which allowed the display to be expanded over a shorter time base. Photographs were taken of the oscilloscope display. The contact diameter was measured by chalking the cladding and measuring the impression left by the projectile with calipers.

COMPARISON OF THE TEST RESULTS AND THE COMPUTED VALUES

The comparison of experimental results with theoretical values gave very good agreement, with the theoretical value being somewhat higher. For the purpose of conservation of space, only a selected number of representative results were included in the illustrations.

Velocity of impact vs. radius of contact for the plates and shells with Lexan and Adiprene coverings are shown in Figs. 6–8. Strain vs. velocity of impact on steel plate with and without coverings are shown in Fig. 9 for a 1 in. radius projectile. Similar results were obtained for impact on an aluminum plate with and without coverings for both the 1 in. and the $\frac{1}{2}$ in. projectiles. Strain vs. various thicknesses of aluminum and steel plates for a 1 in. radius projectile are shown in Figs. 10 and 11, respectively. The bending effect is quite pronounced for the very thin plates. Stress vs. applied load on glass and aluminum shells are shown in Figs. 12 and 13 respectively. All tests were calculated assuming both a hemispherical and a uniform loading with the hemispherical loading giving a higher result.

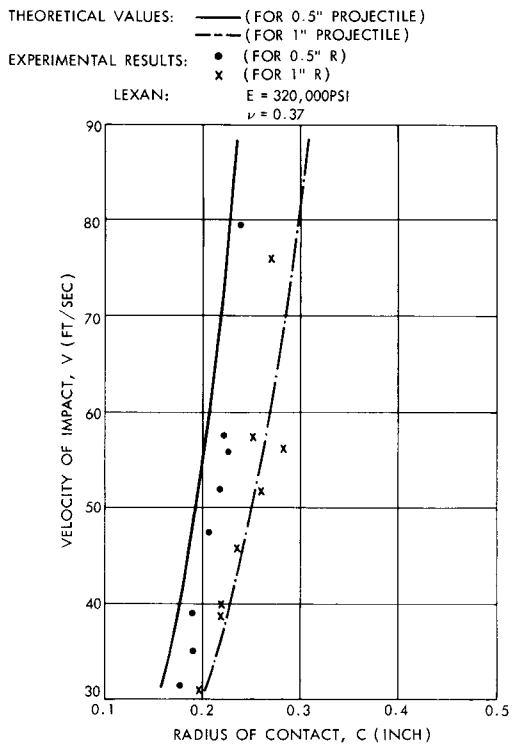

FIG. 6. Velocity of impact vs. radius of contact (Lexan covering).

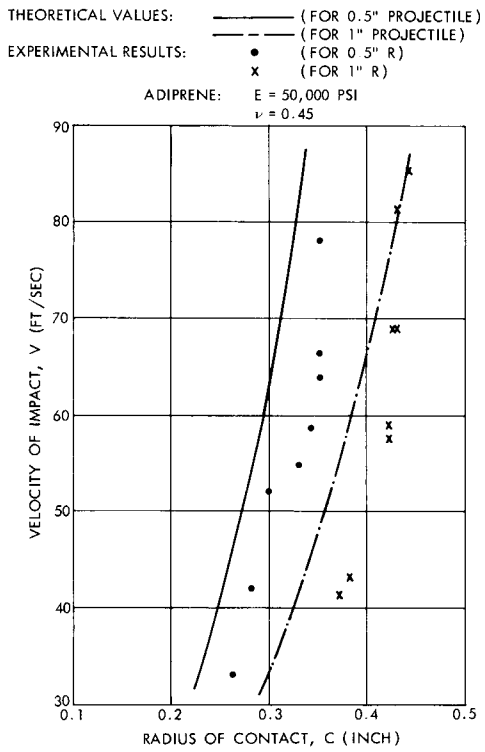

FIG. 7. Velocity of impact vs. radius of contact (Adiprene covering).

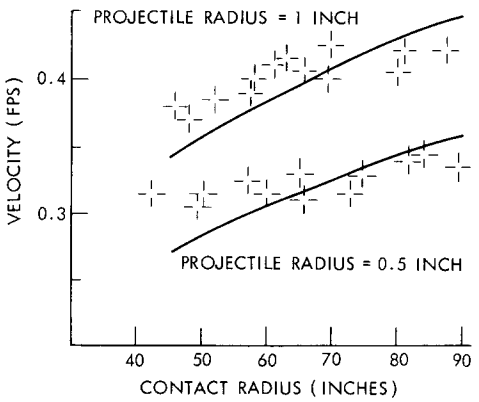

FIG. 8. Observed and calculated contact radius as a function of projectile velocity for shells with Adiprene cladding.

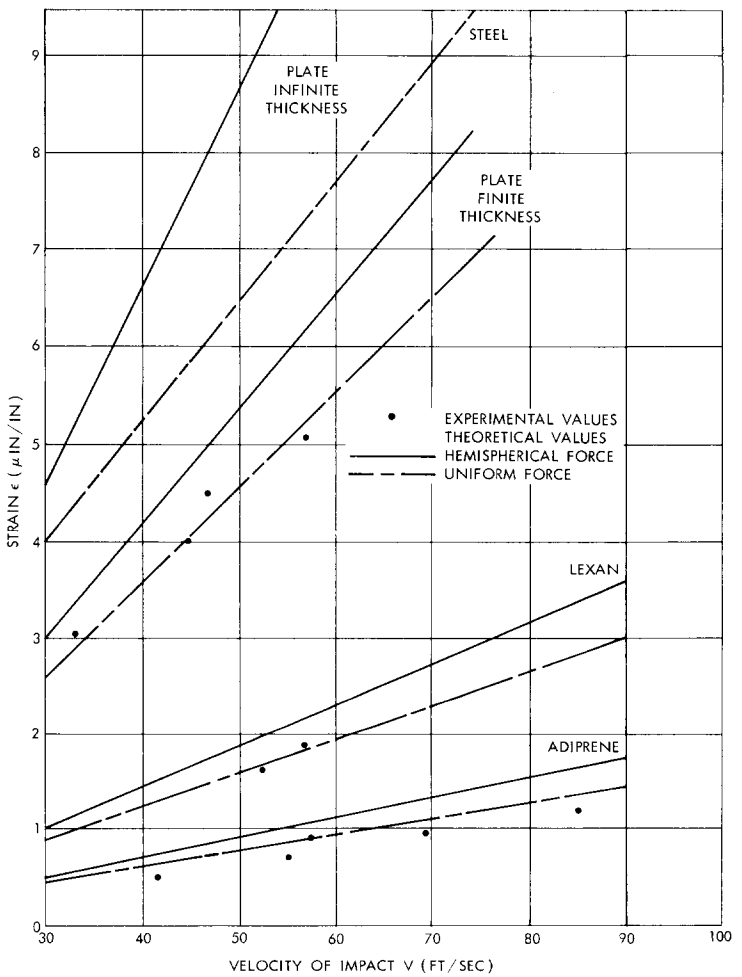

FIG. 9. Strain vs. velocity of impact (1 in. radius projectile).

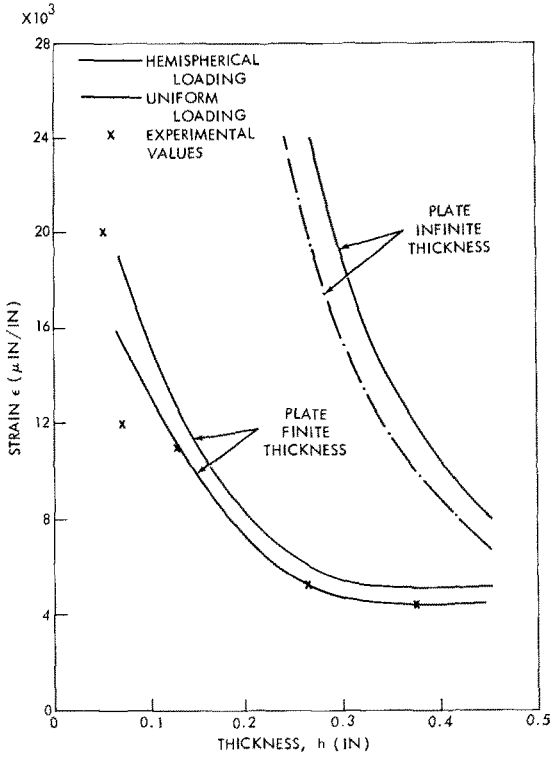

FIG. 10. Strain vs. thickness of plate (Al) (velocity of impact: 33 ft/sec).

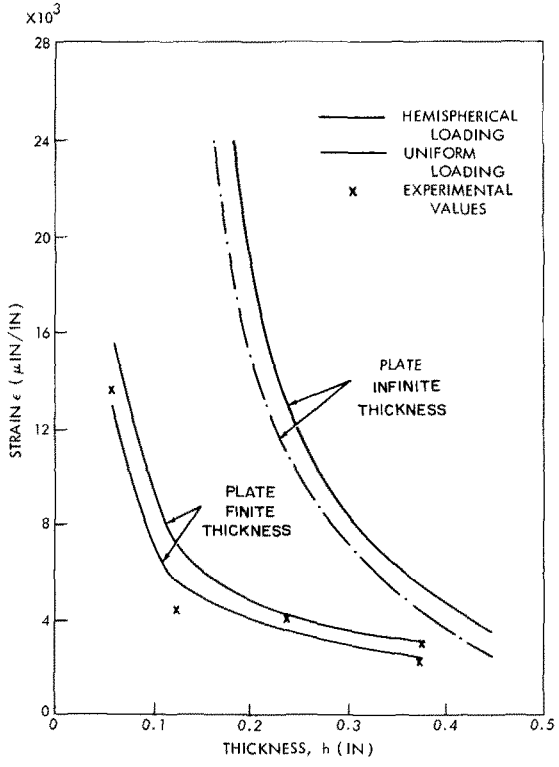

FIG. 11. Strain vs. thickness of plate (steel) (velocity of impact: 33 ft/sec).

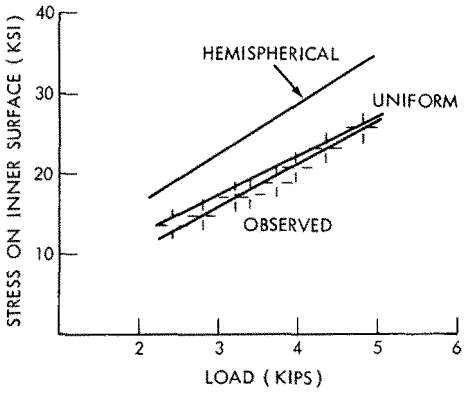

FIG. 12. Stress on inner surface as a function of load distribution for glass shell with Adiprene cladding; projectile radius 1 in.

DISCUSSION AND CONCLUSION

The radius of contact between the projectile and the covering was measured after each impact test. These values were compared with the theoretically calculated values using the Hertz law for the contact of elastic (projectile) and viscoelastic (Adiprene) bodies, and elastic (projectile) and plastic (Lexan) bodies. It was found that there was a reasonable agreement between experimental and theoretical values. This indicates that under proper circumstances it is valid to use the Hertz force–indentation law in problems of impact and it also supports the conclusion that the application of the Hertz law can be extended to the contact of viscoelastic bodies in some instances [2].

In order to compare the experimental results with the theoretical values of the strain for the plate and shell with coverings, compressive forces and radii of contact between projectiles and coverings were first calculated. Then the plate and shell were considered to be subjected to these forces with and without coverings. The values of the stresses were calculated with the aid of a digital computer from the thin plate theory and the thin shell theory of Reissner [10].

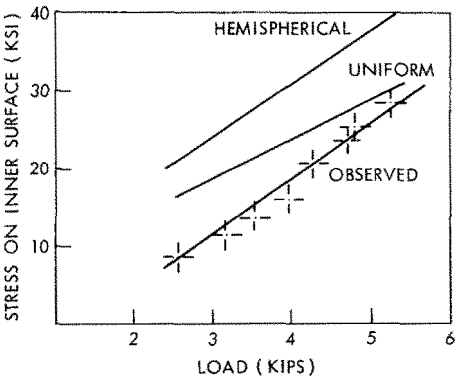

FIG. 13. Stress on inner surface as a function of load distribution for aluminum shell with Adiprene cladding; projectile radius 1 in.

From the comparison it was found that the experimental results were in good agreement with the theoretical values considering the fact that there existed a certain depth of layer of covering between projectile and plate and a possible friction loss between the covering and the plate.

For the different radii of projectiles it was found that even with the same mass and at the same velocity of impact the projectile of larger radius produced a greater compressive force as well as a larger radius of contact between bodies, thus producing a larger strain both theoretically and experimentally.

From an evaluation of the theoretical results for both the hemispherically and uniformly distributed contact pressure, the latter was found to be closer to the experimental results. However, since all of the results are reasonably close, both cases can be used to predict the approximate impact characteristics of thin plates and shells.

It was noticed that under the above conditions all plates and shells tested remained within the elastic range.

From the comparison of plates with and without coverings it was found that Adiprene served as the best mitigator of shock. It reduced the magnitude by a factor of four on the average. Lexan also served as a good mitigator, where a factor of two was obtained.

In addition, experimental tests were also carried out on the plates without coverings where plastic yieldings (a slight permanent set) occurred at the point of contact. Observing the results, the same conclusion can be obtained that the Hertz law is applicable. This also verifies the conclusion reached by Goldsmith [6] that the Hertz law is valid under proper circumstances even when some permanent set is produced.

For a fundamental discussion of the elastic impact of projectiles on plates, the work of Zerner (Ref. [13]) and the experimental work of Tillett (Ref. [14]) should be consulted.

It is further suggested that the problem of large plastic deformation be studied combining the theory of plasticity with some modification of the Hertz law.

Acknowledgments—I would like to thank Dr. Jack E. Goeller for his many valuable suggestions, and Mr. D. S. Chun and Mr. J. R. Camper for their assistance in the calculation and testing.

REFERENCES

[1] H. Hertz, *Miscellaneous Papers*, the English translation, p. 146. Jones and Scott (1965).
[2] R. M. Davis, The determination of static and dynamic yield stresses using a steel ball. *Proc. R. Soc.* **A197**, 416–432 (1949).
[3] A. E. H. Love, *The Mathematical Theory of Elasticity*. Dover (1927).
[4] Y. M. Tsai and H. Kolsky, A study of the fractures produced in glass blocks by impact. *J. Mech. Phys. Solids* **15**, 263–278 (1967).
[5] C. V. Raman, On some applications of Hertz's theory of impact. *Phys. Rev.* **15**, 277–284 (1920).
[6] W. Goldsmith, Impact at Intermediate Velocities Contact Phenomena, NAVWEPS Report 8088, U.S. Naval Ordnance Test Station, China Lake, California (1963).
[7] S. Timoshenko and J. N. Goodier, *Theory of Elasticity*, 2nd edition, pp. 372–384. McGraw-Hill (1951).
[8] W. Goldsmith, *Impact*, pp. 83–91. Edward Arnold (1960).
[9] S. Timoshenko and S. Woinowsky-Krieger, *Theory of Plates and Shells*, 2nd edition, pp. 79–113. McGraw-Hill (1959).
[10] E. Reissner, Stresses and small displacements of shallow spherical shells–II. *J. Math. Phys.* **25**, 279–300 (1964).
[11] *ASM Handbook*, Vol. 1, p. 64 (1961).
[12] W. M. Hinckley and F. P. Stecher, Medium Strain Rate, Compression Testing of Selected Plastic Materials, NOLTR 67–178, Naval Ordnance Laboratory, White Oak, Maryland (1967).

[13] E. ZENER, Elastic impact of projectile on plates. *Phys. Rev.* **59**, 669 (1941).
[14] J. P. A. TILLETT, Fracture of glass by spherical indenters. *Proc. Phys. Soc.* **67**, 677 (1954).

(*Received* 6 *January* 1970; *revised* 3 *June* 1970)

Абстракт—Даются теоретические зависимости и экспериментальные данные для столкновения снарядов, с головкоч в форме полущария, с полусферическими оболочками и квадратными пластинками, с защитным покритием или без. Расщирение статической контактной задачи Герца и закон внедрения силы вместе с теориями пластинок и оболочек дает возможность определить теоретические зависимости для расчета распределения напряжений. Сравниваются экспериментально теоретические предусмотрения путем использования воздушного пульверизатора, для удара стальных снарядов, с головкой в форме полушария, в стекляные и алюминиевые полусферические оболочки и изготовленные с таких же материалов квадратные пластинки, с вязкоупругими/ полиуретан/ и пластическим /поликарбонат/ покрытием, или без. Приводятся измерения деформаций датчиками деформаций, расположенными на свободной стороне пластинки или оболочки, непосредственно под точкой удара. Получаются умеренная сходимость между результатами из расчетов и данными из экспериментов.